Available online at http://jprm.sms.edu.pk/
Journal of Prime Research in Mathematics, 21(1) (2025), 82-100

Journal of Prime Research in Mathematics

Mathematical Modeling of Anticancer Drugs Using Distance-based Topological Indices

Abdulrahman Ali Alsolami[a], Muhammad Faisal Nadeem[b,*]

[a]*Department of Mathematics, Faculty of Science, King Abdulaziz University, P.O.Box:80203 Jeddah: 21589, Kingdom of Saudi Arabia.*

[b]*Department of Mathematics, COMSATS University Islamabad, Lahore Campus, Lahore 54000, Pakistan.*

Abstract

We examine the suitability of distance-based topological indices in modeling and forecasting the physicochemical properties of a selection of key drugs like Trastuzumab, Tamoxifen, paclitaxel, Ibritumomab, Gemcitabine, Fluorouracil (5-FU), and Doxorubicin. Four different indices, Mostar, Szeged, TrinajstiA, and Padmakar-Ivan (PI), were derived from molecular graphs for each drug. Quadratic models demonstrated appreciable correlations between these indices and principal physicochemical properties, such as molecular weight and melting points. Topological indices are found to effectively forecast physicochemical properties, making them valuable aids in drug design, optimization, and discovery. The mathematical models shed light on structural complications that affect drug efficacy and pharmacokinetics, proving graph-theoretical methods effective in predicting these effects.

Keywords: Mathematical modeling, mostar index; Szeged index; trinajstić index, Padmakar-Ivan index, Drug discovery.

1. Introduction

The role of pharmaceuticals and drugs in modern-day medicine highlights the importance of extensive studies on drug discovery, synthesis, and analysis [1, 2]. This research takes on greater relevance when quantitative techniques, such as topological indices, are employed, which yield numerical descriptors based on chemical structures described using molecular graphs [3, 4]. Topological indices enable the interpretation of physicochemical properties [5], biological activity [6, 7], and structural characteristics of drug compounds

*Corresponding author
Email addresses: aalsolami1@kau.edu.sa (Abdulrahman Ali Alsolami), mfaisalnadeem@ymail.com (Muhammad Faisal Nadeem)

Received : 23 June 2025*; Accepted:* 19 September 2025*; Published Online:* 22 September 2025.

[8]. This research focuses on the topological indices of several leading drugs, including Trastuzumab, Tamoxifen, Paclitaxel, Ibritumomab, Gemcitabine, Fluorouracil, Doxorubicin, and 5-Fluorouracil. All these drugs have extensive clinical usage, and each has a unique molecular structure that affects its efficacy and pharmacokinetics.

Trastuzumab is a monoclonal antibody that is widely used for the targeted treatment of breast cancer, especially HER2-positive cancer [9, 10]. It specifically binds to the extracellular domain of the HER2 receptor, halting cancer cell proliferation through various mechanisms, including receptor internalization and antibody-dependent cytotoxicity by immune cells. Clinically, Trastuzumab is found to considerably enhance patient outcomes when used in combination with chemotherapy or as a standalone treatment. Physicochemically, the molecular size and structural complexity of Trastuzumab are significant and important to its pharmacological profile and therapeutic effect.

Tamoxifen is a selective estrogen receptor modulator that has been used frequently for treatment and prevention of breast cancer that is estrogen receptor-positive [11]. Its action consists largely of competitive inhibition of the binding between estrogen and its receptor, thereby preventing the proliferation of tumor cells. It also has a prophylactic application in breast cancer risk reduction within high-risk individuals. It is structurally hydrophobic and exhibits significant stereochemistry, which significantly affects its biodistribution and bioavailability.

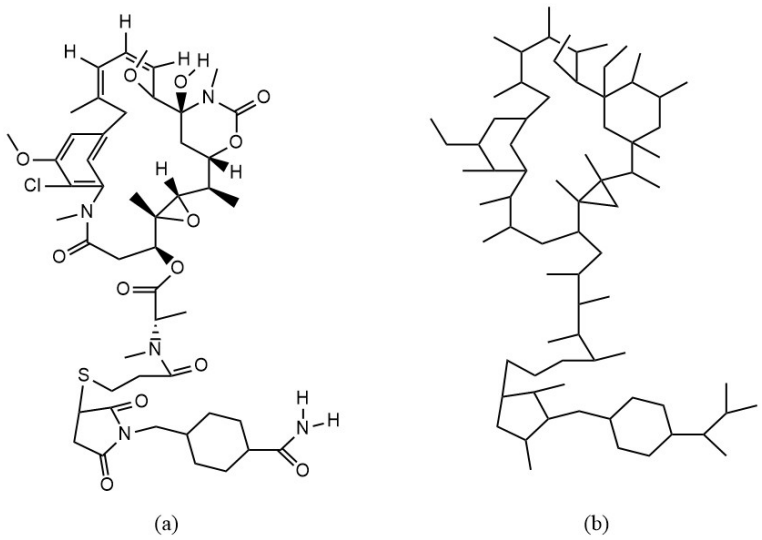

(a) (b)

Figure 1: Trastuzumab

Paclitaxel, isolated from the bark of the tree Taxus brevifolia, is an antimitotic compound that is widely used in oncology for the treatment of ovarian, breast, lung, and pancreatic cancers [12]. Paclitaxel stabilizes microtubules, thereby interfering with normal processes during mitosis and inducing apoptosis in cancer cells [13]. Its clinical utility is compounded by its broad range of anti-tumor activity and its use as an initial-line chemotherapy treatment. The multi-ring, high-molecular-weight nature of Paclitaxel's complex molecule affects solubility and requires considerations for formulation.

Ibritumomab is a radioimmunotherapeutic monoclonal antibody targeting the CD20 antigen, most commonly used to treat non-Hodgkin's lymphoma [14]. It is radiolabeled using isotopes like Yttrium-90 and, by delivering cytotoxic radiation directly to neoplastic cells, causes less systemic toxicity than traditional chemotherapy. The therapeutic activity of the drug is based on its radioisotope linkage and molecular specificity, which directly impact its pharmacodynamics and clinical effects.

Gemcitabine is a nucleoside analogue that is highly effective against various malignancies, including pancreatic, breast, ovarian, and lung cancers [15]. Its action is through incorporation into the DNA during replication, leading to premature DNA elongation termination and induction of apoptosis [16]. The pharmaceutical agent exhibits advantageous pharmacokinetic properties, specifically characterized by efficient

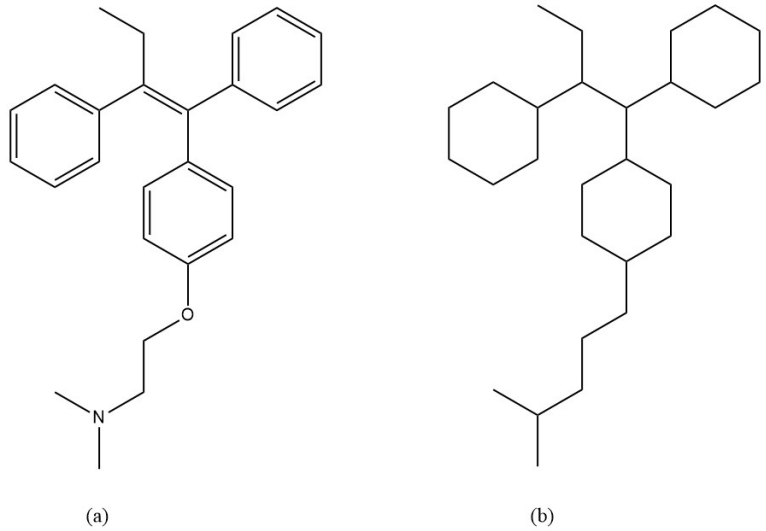

Figure 2: Trastuzumab

intracellular uptake and an elevated phosphorylation rate, thereby enhancing its therapeutic effectiveness. Its structural analogy to cytidine is pivotal in determining its biological activity and metabolic processing.

Fluorouracil, or 5-FU, is a fluoropyrimidine antimetabolite widely used in the treatment of malignancies within the colon, stomach, pancreas, and breast [17]. Therapeutically, its actions rely on the inhibition of thymidylate synthase, thereby interfering with the formation of thymidine nucleotides and causing DNA damage, which leads to apoptosis. Clinically, Fluorouracil is incorporated into various treatment regimens, often in combination with other cytotoxic drugs or radiotherapy, to enhance treatment outcomes. The physicochemical properties of the substance, typified by its relative simplicity and small size, enable it to invade neoplastic cells. The substance 5-Fluorouracil (5-FU), chemically synonymous with the above-mentioned Fluorouracil, is particularly notable for its high clinical usage rate and its status as a key component in chemotherapy regimens for most types of cancer. The drug's pharmacological activity is centered on its antimetabolite activity, which causes significant disruption in the formation and functioning of nucleic acids. The structural simplicity of 5-FU enhances its bioavailability, allowing it to be incorporated into a wide range of chemotherapeutic regimens.

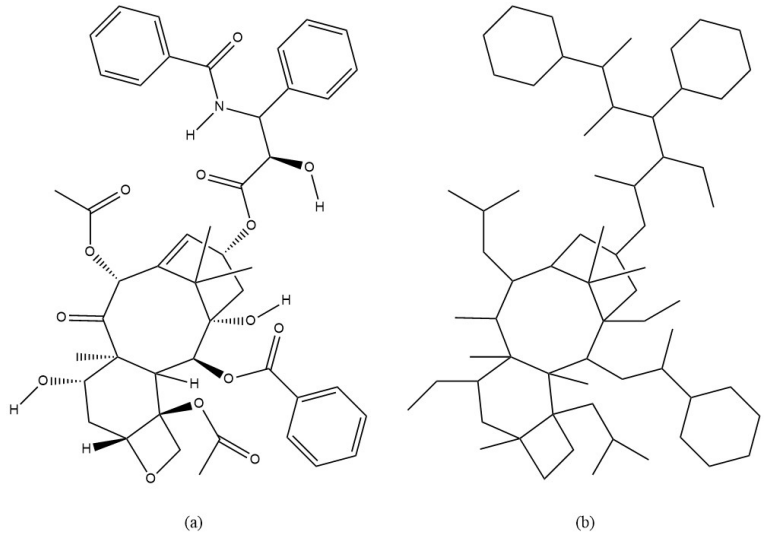

Figure 3: Paclitaxel

The anthracycline antibiotic Doxorubicin is renowned for its high anti-neoplastic activity and has been widely used against leukemias, lymphomas, and solid tumors, such as breast, ovarian, and lung cancers [18]. The underlying mechanism is based on intercalation into DNA strands, inhibition of topoisomerase II, and the generation of free radicals, and these three mechanisms work synergistically to produce cytotoxic effects against tumor cells. Although Doxorubicin is highly effective, its clinical use is limited by dose-dependent cardiotoxicity, and close monitoring and dosage adjustments may be required. The compound's planar aromatic ring system significantly impacts its capacity for intercalation, and hence, its biological activity. The mentioned pharmacological agents are important therapeutic compounds with varied uses in oncology,

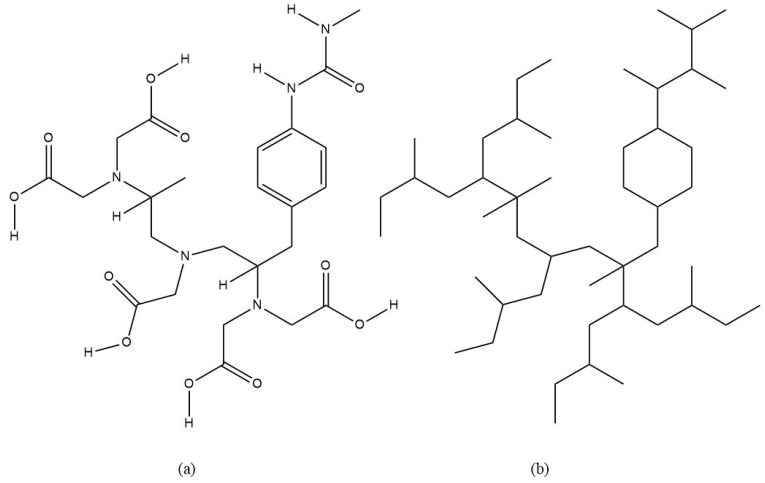

Figure 4: Ibritumomab

characterized by innovative topological structures and strong pharmacological effects. The application of topological indices to assess drug yields provides important information regarding physicochemical properties, which may be instrumental in better drug design, optimization, and clinical use strategies. The purpose of this article is to discuss and review the significance of topological indices, which are important for drug research and development.

Topological indices are significant in pharmaceutical research and drug discovery, as they provide quantitative representations of molecular structure, enabling the prediction of pharmacological activities, biological effects, and physicochemical properties [19, 20, 21]. They are of significant utility in quantitative structure-activity relationships, enabling scientists to project how changes in the structure of a molecule affect the effectiveness, toxicity, and bioavailability of a drug. They reduce complex molecular shapes into quantitative figures, speeding up the process of drug design, optimization, and screening, ultimately accelerating the identification and development of candidate drugs. Distance-based topological index applications are widespread in pharmaceutical chemistry and molecular biology, extracting useful quantitative structure-activity relationships (QSARs) that describe molecular structure, reactivity, and biological activities. They quantify molecular structure in terms of interatomic distances, playing a significant role in predicting drugs by correlating the architecture of the molecule with its pharmacological effectiveness and toxicological properties. They are essential in QSAR/QSPR research for predicting physicochemical properties, including boiling point, melting point, stability, and solubility of the drug molecule. Distance-based indexes also identify structural similarities or dissimilarities in sets of molecular datasets with ease, allowing for the clustering and categorization of chemical compounds. In medicinal chemistry, index-based predictions of the binding affinity of a potential drug molecule with a biological receptor guide the process of modifying and optimizing the molecule. Distance-based topological indexes also play a significant role in modeling the interaction of molecules, predicting bioactivity, environmental impact, and developing compounds with increased therapeutic potency and fewer side effects.

Topology-derived numerical descriptors, known as topological indices (TIs), have become essential for

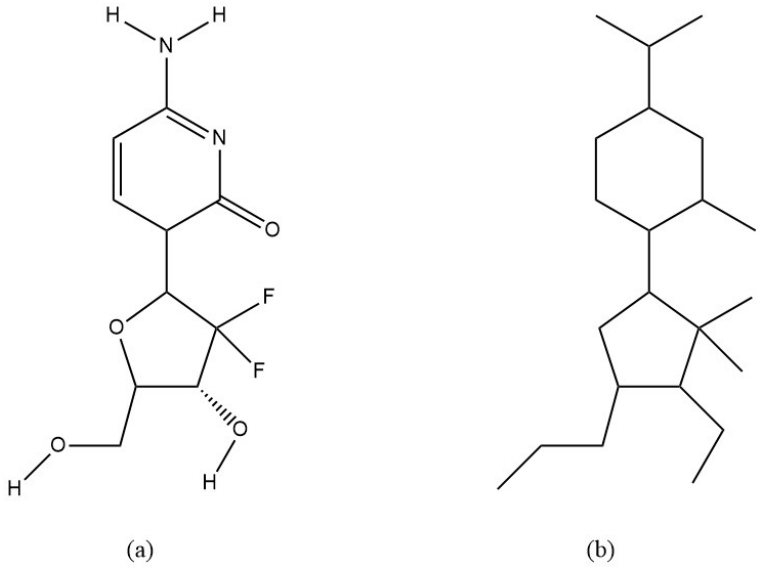

Figure 5: Gemcitabine

drug QSAR/QSPR research, as they contain structural information in numerical terms. Degree-based indices derived from vertex degrees are among the most popular. A good example is the use of the Randic connectivity index in predicting drug activities and druglike pharmacokinetics [22]. Gao et al. calculated several degree-based indexes for an anticancer drug formulation family of smart polymers and illustrated how these can be used to predict the physical attributes, chemical reactivity, and biological activity of the drug–polymer conjugates [23]. Rani & Ali studied the indices of polysaccharides. Shanmukha et al. established thirteen degree-based topological indexes for anticancer drugs and conducted a QSPR analysis, finding that index values have a strong correlation with the physicochemical attributes of the drugs [25].

Degree-based indices have also played instrumental roles in descriptor modeling of bioactivities of small-molecule drugs. Kirmani et al. studied certain antiviral drugs and computed degree-based and neighborhood degree-sum indices using the M-polynomial approach [26]. Suay-García et al. demonstrated that an index derived from vertex classes can be an efficient descriptor for antibacterial potency in quinolones [27]. Ding et al. computed the indices of networks [28]. Rasheed et al. proposed modified Randić indices for certain series of drugs against infection and demonstrated through regression models that the new indices have a strong correlation with attributes such as molecular weight and refractive index [29].

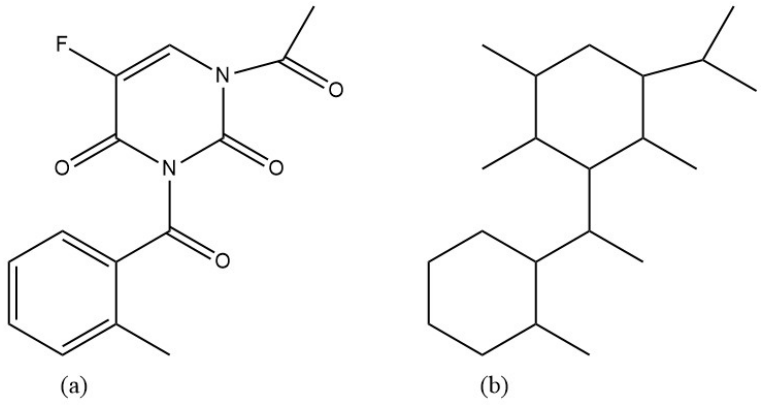

Figure 6: Fluorouracil

Several thematic patterns are evident in contemporary literature. One of these is the use of degree-based indicators in the discovery of anticancer drugs. Most anticancer QSAR research utilizes indicators such as

the Zagreb numbers and Randić index to capture descriptors of cytotoxic potency. Zheng et al. studied hyaluronic acid–paclitaxel conjugates and calculated a series of topological indicators using an edge-partition approach [30]. Yousaf and Shahzadi (2024) employed degree-based indicators to model anti-cancer potency in the context of drug repurposing. These authors developed QSPR models for a diverse selection of "non-cancer" drugs and successfully identified multiple existing drugs with high predicted anti-cancer potency [31].

In addition to vertex-degree parameters, distance-based topological descriptors have become increasingly popular in drug research for simulating physicochemical and ADME properties. Traditional distance-based descriptors, such as the Wiener index (the sum of all the shortest path lengths in a graph of molecules), were among the first QSPR parameters and remain influential in present-day research. In the most recent decade, new distance-derived indexes have been developed to more accurately account for the complexity of molecules, as well as 3D considerations.

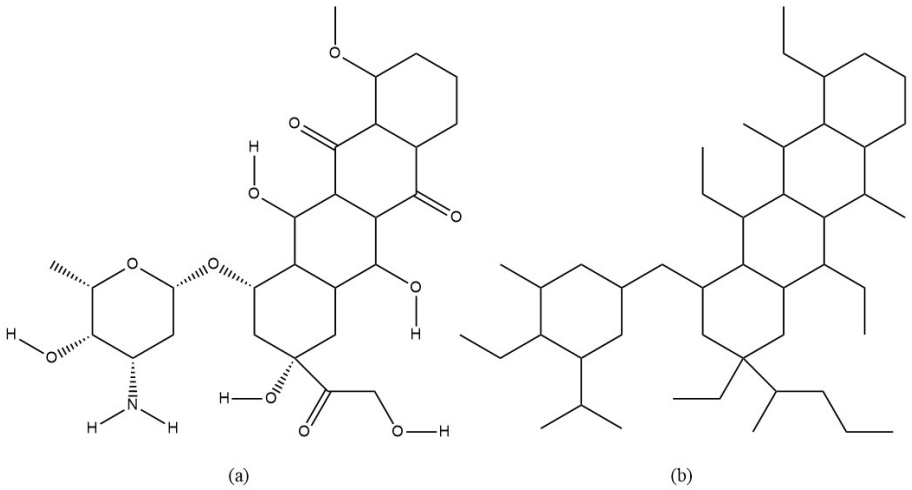

Figure 7: Doxorubicin

Topological indices are essential mathematical tools in chemistry, offering numerical descriptors that summarize the structural aspects of chemical molecules [34]. One of the most widely used and earliest of these is the Wiener index, introduced by Wiener in 1947 for calculating boiling points of paraffin molecules. The Wiener index is the sum of all the distances along the shortest paths between vertex pairs in the molecular graph, and it has been found to be highly correlated with physicochemical descriptors, such as boiling point, as well as other properties, including viscosity and surface tension.

In the 1990s, attempts to generalize distance indices to cyclic graphs led to the introduction of the Szeged index (Sz) by Gutman [35] and subsequent development in terms of Szeged matrices [36]. Szeged-type indices partition the graph at every edge and agree with W on trees. Another distance invariant, the Padmakar-Ivan (PI) index, was initially introduced as a bond-centered index; vertex and edge variants have been formulated ever since [37]. More recent improvements involve a modified Wiener index with peripheral distances at its core [38] and the revised Wiener index of Randic, which addresses Szeged's deficiency for the case of cyclic structures [39]. Most recently, an innovative distance-based metric, termed the Mostar index [40], was introduced to calculate distance disparity in graphs by summing the imbalance of vertex distances across each bond, representing the notion of distance-unbalancedness [41].

2. Materials and Methods

This research examines the distance-based topological indices of several pharmacologically relevant drugs, including Trastuzumab, Tamoxifen, Paclitaxel, Ibritumomab, Gemcitabine, Fluorouracil (5-FU), and Doxorubicin. These drugs have been chosen on account of their extensive application and research interest in the field of onc

The structures of the chosen drugs, including Trastuzumab, Tamoxifen, Paclitaxel, Ibritumomab, Gemcitabine, Fluorouracil (5-FU), and Doxorubicin, were obtained from well-documented chemical databases such as PubChem, ChemSpider, and DrugBank. The molecules were downloaded in standard formats, including SDF (Structure Data File) and MOL (MDL Molfile), to facilitate compatibility and standardization during computational processing.

These molecular structures were then transformed into respective graphs of molecules where atoms were represented as vertices (nodes) and chemical bonds as edges. The hydrogen atoms were strategically omitted from the graphs for ease of computation and to portray the core connectivity of the molecules.

The molecular structure of Trastuzumab is shown in Figure 1(a) and its corresponding molecular graph in Figure 1(b). Similarly, the structure and graph for Tamoxifen are illustrated in Figure 2(a) and Figure 2(b), for Paclitaxel in Figure 3(a) and Figure 3(b), for Ibritumomab in Figure 4(a) and Figure 4(b), for Gemcitabine in Figure 5(a) and Figure 5(b), for Fluorouracil (5-FU) in Figure 6(a) and Figure 6(b), for Doxorubicin in Figure 7(a) and Figure 7(b).

Four unique distance-based topological indices were computed: Trinajstic descriptor, Mastar descriptor, Szeged descriptor, and PI descriptor. These descriptors measure various features of the topology of molecules, including distance-based attributes, and capture variations in vertex and edge distribution.

The indices are mathematically defined as follows:

Trinajstić Descriptor (NT):

$$NT(\mathbb{M}) = \sum_{r,s \in V(\mathbb{M})} (\varsigma_r - \varsigma_s)^2, \tag{2.1}$$

where ς_r and ς_s represent the number of vertices closer to vertex r than to vertex s and vice versa, respectively.

Mostar Descriptor (Mo):

$$Mo(\mathbb{M}) = \sum_{rs \in E(\mathbb{M})} |\varsigma_r - \varsigma_s|, \tag{2.2}$$

where the summation runs over all edges of the graph $\mathbb{M}$.

Szeged Descriptor (Sz):

$$Sz(\mathbb{M}) = \sum_{rs \in E(\mathbb{M})} \varsigma_r \varsigma_s, \tag{2.3}$$

calculated over all edges $rs \in E(\mathbb{M})$.

PI Descriptor (PI):

$$PI(\mathbb{M}) = \sum_{rs \in E(\mathbb{M})} (\varsigma_r + \varsigma_s), \tag{2.4}$$

calculated the sum of vertex counts ς_r and ς_s for all edges in $\mathbb{M}$.

3. Results and Discussion

Distance-based topological descriptors, such as the Trinajstić descriptor (NT), Mostar descriptor (Mo), Szeged descriptor (Sz), and Padmakar-Ivan (PI) descriptor, were calculated for the structures of the anticancer drugs: Trastuzumab, Tamoxifen, Paclitaxel, Ibritumomab, Gemcitabine, Fluorouracil (5-FU), and Doxorubicin. Consistent with the methodological scope, melting point regressions are reported only for small molecules. Biologics are excluded from MP fitting because their thermal transitions correspond to protein unfolding or decomposition rather than crystal melting.

3.1. Results of Trastuzumab

We compute four distance-based topological indices—Trinajstic (NT), Mostar (Mo), Szeged (Sz), and Padmakar–Ivan (PI)—for Trastuzumab's molecular graph here. These indices provide valuable insights into the molecular structure's structural topology through quantitative measurements of various aspects

of atomic connectivity and distance distribution. The computation is performed for the molecular graph, where atoms are represented as vertices and bonds as edges. However, hydrogen atoms are ignored to focus on the fundamental molecular framework. Each index is calculated using graph-based formulations, and results capture the underlying complexity and irregularity present in Trastuzumab's molecular structure.

Mostar Index

The Mostar index for Trastuzumab's molecular graph is calculated to be 4000, indicating high structural asymmetry between vertex distances across edges. This index is calculated as the sum of all the absolute vertex distance differences $|n_u - n_v|$ for all edges uv in the graph, where n_u and n_v are the number of vertices closer to vertex u and v respectively.

Table 1: Edge-wise values of n_u and n_v for the edges in the molecular graph of Trastuzumab

Edge	n_u	n_v	Edge	n_u	n_v	Edge	n_u	n_v	Edge	n_u	n_v
(n_{v_0}, n_{v_1})	22	48	(n_{v_0}, n_{v_5})	18	23	(n_{v_0}, n_{v_8})	73	0	(n_{v_1}, n_{v_2})	21	49
(n_{v_1}, n_{v_9})	73	0	$(n_{v_2}, n_{v_{31}})$	20	51	(n_{v_3}, n_{v_4})	52	19	$(n_{v_3}, n_{v_{10}})$	72	1
$(n_{v_3}, n_{v_{12}})$	20	51	(n_{v_4}, n_{v_5})	53	19	(n_{v_4}, n_{v_6})	73	0	(n_{v_5}, n_{v_7})	73	0
$(n_{v_{10}}, n_{v_{11}})$	73	0	$(n_{v_{12}}, n_{v_{13}})$	73	0	$(n_{v_{12}}, n_{v_{14}})$	70	3	$(n_{v_{12}}, n_{v_{18}})$	22	48
$(n_{v_{14}}, n_{v_{15}})$	21	49	$(n_{v_{15}}, n_{v_{16}})$	73	0	$(n_{v_{15}}, n_{v_{17}})$	18	51	$(n_{v_{17}}, n_{v_{19}})$	3	70
$(n_{v_{18}}, n_{v_{19}})$	17	52	$(n_{v_{19}}, n_{v_{20}})$	73	0	$(n_{v_{19}}, n_{v_{21}})$	20	51	$(n_{v_{21}}, n_{v_{22}})$	73	0
$(n_{v_{21}}, n_{v_{23}})$	21	51	$(n_{v_{23}}, n_{v_{24}})$	73	0	$(n_{v_{23}}, n_{v_{25}})$	73	0	$(n_{v_{23}}, n_{v_{26}})$	22	49
$(n_{v_{26}}, n_{v_{27}})$	73	0	$(n_{v_{26}}, n_{v_{28}})$	73	0	$(n_{v_{26}}, n_{v_{29}})$	23	48	$(n_{v_{29}}, n_{v_{30}})$	43	30
$(n_{v_{29}}, n_{v_{44}})$	53	18	$(n_{v_{30}}, n_{v_{45}})$	44	29	$(n_{v_{31}}, n_{v_{32}})$	68	5	$(n_{v_{31}}, n_{v_{33}})$	22	48
$(n_{v_{32}}, n_{v_{35}})$	20	50	$(n_{v_{33}}, n_{v_{34}})$	17	53	$(n_{v_{34}}, n_{v_{36}})$	68	5	$(n_{v_{34}}, n_{v_{40}})$	20	50
$(n_{v_{35}}, n_{v_{36}})$	19	51	$(n_{v_{35}}, n_{v_{37}})$	72	1	$(n_{v_{36}}, n_{v_{39}})$	73	0	$(n_{v_{37}}, n_{v_{38}})$	73	0
$(n_{v_{40}}, n_{v_{41}})$	73	0	$(n_{v_{40}}, n_{v_{42}})$	19	51	$(n_{v_{42}}, n_{v_{43}})$	73	0	$(n_{v_{42}}, n_{v_{44}})$	19	52
$(n_{v_{45}}, n_{v_{46}})$	73	0	$(n_{v_{45}}, n_{v_{47}})$	46	27	$(n_{v_{47}}, n_{v_{48}})$	73	0	$(n_{v_{47}}, n_{v_{49}})$	48	25
$(n_{v_{49}}, n_{v_{50}})$	73	0	$(n_{v_{49}}, n_{v_{51}})$	50	23	$(n_{v_{51}}, n_{v_{52}})$	73	0	$(n_{v_{51}}, n_{v_{53}})$	52	21
$(n_{v_{53}}, n_{v_{54}})$	53	20	$(n_{v_{54}}, n_{v_{55}})$	54	19	$(n_{v_{55}}, n_{v_{56}})$	55	18	$(n_{v_{56}}, n_{v_{57}})$	57	14
$(n_{v_{56}}, n_{v_{59}})$	58	2	$(n_{v_{57}}, n_{v_{58}})$	73	0	$(n_{v_{57}}, n_{v_{60}})$	58	14	$(n_{v_{59}}, n_{v_{61}})$	57	14
$(n_{v_{60}}, n_{v_{61}})$	14	2	$(n_{v_{60}}, n_{v_{63}})$	62	11	$(n_{v_{61}}, n_{v_{62}})$	73	0	$(n_{v_{63}}, n_{v_{64}})$	63	10
$(n_{v_{64}}, n_{v_{65}})$	66	7	$(n_{v_{64}}, n_{v_{66}})$	66	7	$(n_{v_{65}}, n_{v_{68}})$	66	7	$(n_{v_{66}}, n_{v_{67}})$	66	7
$(n_{v_{67}}, n_{v_{69}})$	66	7	$(n_{v_{68}}, n_{v_{69}})$	66	7	$(n_{v_{69}}, n_{v_{70}})$	69	4	$(n_{v_{70}}, n_{v_{71}})$	73	0
$(n_{v_{70}}, n_{v_{72}})$	71	2	$(n_{v_{72}}, n_{v_{73}})$	73	0	$(n_{v_{72}}, n_{v_{74}})$	73	0			

As reflected in Table 1, a number of edges have high contributions to the overall index because there exist large differences between local neighborhood sizes of their incident vertices. For instance, for edge (v_1, v_9), $n_u = 73$ and $n_v = 0$ leading to $|n_u - n_v| = 73$ which is the maximum single edge contribution. Similarly, other such high contributing edges are (v_1, v_8), (v_{11}, v_{12}), and (v_{15}, v_{16}) all contributing $|n_u - n_v| = 73$. Further, moderate contributing edge are (v_1, v_6), $n_u = 18$ and $n_v = 23$ leading to $|n_u - n_v| = 5$ and for (v_{14}, v_{15}) $n_u = 21$ and $n_v = 49$ leading to $|n_u - n_v| = 28$.

These variations highlight the uneven distribution of vertex distances in Trastuzumab's graph, directly impacting the size of the Mostar index and indicating the heterogeneity and complexity of the molecule's topology.

Szeged Index

The Szeged index for the Trastuzumab molecular graph is found to be 41155. For Trastuzumab, numerous contributing edges make a significant contribution to the overall Szeged index due to the high product $n_u \cdot n_v$. An example is the edge (v_1, v_2) which has $n_u = 21$ and $n_v = 49$ and will therefore contribute 1029, while v_{12}-v_{14} has $n_u = 70$ and $n_v = 3$ and contributes 210. High Szeged values mainly come from those edges whose endpoints have high vertex partitions, for example, (v_3, v_4), which has $n_u = 52$ and $n_v = 19$ contributing 988,

and (v_4, v_5), which has $n_u = 53$ and $n_v = 19$ contributing 1007. The high Szeged index value is an indication of an overall high Szeged index because of the extensive and lopsided distribution of vertex distances within the graph corresponding to Trastuzumab's complex branched topology. The index effectively represents the distance between atoms in the molecular skeleton and has been found to serve as an indicator of spatial complexity in molecules.

Trinajstić Index

The Trinajstić index for Trastuzumab's molecular graph is $NT(\mathbb{M}) = 2{,}824{,}802$. This is derived from calculating the square of differences between the number of vertices nearer to each vertex r and s for all pairs $\{r, s\} \in V(\mathbb{M})$.

A number of representative vertex pairs account for a considerable portion of the overall index because some neighborhood sizes differ significantly from one another. For example, pair $\{v_1, v_9\}$ has $\varsigma_{v_1} = 73$ and $\varsigma_{v_9} = 0$ and therefore makes a contribution of $(73 - 0)^2 = 5329$. Likewise, pair $\{v_3, v_4\}$ contributes $(52-19)^2 = 1089$ and pair $\{v_0, v_8\}$, where $\varsigma_{v_0} = 73$ Moderate contributions are seen in $\{v_0, v_2\}$ and $\{v_0, v_{10}\}$, whose respective squared differences are 729 and 961. Pairs $\{v_0, v_6\}$ have an exceptionally small difference, which only gives $(20 - 21)^2 = 1$. These pairwise contributions cumulatively account for the high overall magnitude of Trinajstić index, which describes the high heterogeneity and spatial pattern of vertices in Trastuzumab's molecular graph.

Padmakar–Ivan (PI) Index

The Padmakar–Ivan (PI) index for the molecular graph of Trastuzumab is 5,604. The index is derived from summing values for $\varsigma_r + \varsigma_s$ for all $rs \in E(\mathbb{M})$. For Trastuzumab, numerous factors contribute significantly to the PI index. The edge (v_1, v_2) contributes $21 + 49 = 70$, while (v_4, v_5) contributes $53 + 19 = 72$. Edges like (v_0, v_8) and (v_1, v_9), with one having $\varsigma = 73$ and the other having $\varsigma = 0$, each have high contributions equal to 73. The overall PI index represents the total number of neighborhood sizes for all edges and provides an indication of the distribution density of atom clusters in the molecular graph. For Trastuzumab, an index value of 5604 implies a dense and highly connected branching pattern, which is typical for large biomolecules with intricate structural patterns.

3.2. Results of Doxorubicin

We calculate here the Mostar, Szeged, Trinajstić and Padmakar–Ivan (PI) indices for Doxorubicin's molecular graph from its topological framework. These distance-based indices describe several structural aspects of the molecule in terms of vertex distances and edge connections.

Mostar Index

The Mostar index for Doxorubicin's molecular graph is found to be 1518. This index measures the total sum $|n_u - n_v|$ for all edges. A few edges illustrate notable vertex neighborhood imbalance. For example, (v_0, v_1) has a contribution of $|4 - 40| = 36$ and (v_0, v_6) has a contribution of $|43 - 1| = 42$, which reflect the branching nature of the molecule. The entire list of neighborhood values for each edge employed in computation is given in Table 2.

Szeged Index

The Szeged index for Doxorubicin is determined to be 10,295. This descriptor sums the products of the vertices that are nearer to each end of an edge. Large, balanced neighborhood sizes are given considerable weight. For example, the edge (v_1, v_2) which has $n_u = 26$ and $n_v = 18$ has a contribution $26 \cdot 18 = 468$ and (v_2, v_3) which has $n_u = 42$ and $n_v = 2$ has a contribution of 84. The Szeged index is indicative of how vertex distances are spread throughout the molecule, and its size for Doxorubicin is in agreement with a moderately branched shape, as seen in Table 2.

Table 2: Edge-wise values of n_u and n_v for the edges in the molecular graph of Doxorubicin

Edge	n_u	n_v	Edge	n_u	n_v	Edge	n_u	n_v	Edge	n_u	n_v
(n_{v_0}, n_{v_1})	4	40	(n_{v_0}, n_{v_5})	42	2	(n_{v_0}, n_{v_6})	43	1	(n_{v_1}, n_{v_2})	26	18
(n_{v_1}, n_{v_8})	9	35	(n_{v_2}, n_{v_3})	42	2	$(n_{v_2}, n_{v_{11}})$	9	35	(n_{v_3}, n_{v_4})	40	4
(n_{v_4}, n_{v_5})	18	26	(n_{v_6}, n_{v_7})	44	0	(n_{v_8}, n_{v_9})	9	35	$(n_{v_8}, n_{v_{20}})$	44	0
$(n_{v_9}, n_{v_{10}})$	26	18	$(n_{v_9}, n_{v_{12}})$	16	28	$(n_{v_{10}}, n_{v_{11}})$	35	9	$(n_{v_{10}}, n_{v_{15}})$	16	28
$(n_{v_{11}}, n_{v_{22}})$	44	0	$(n_{v_{12}}, n_{v_{13}})$	16	28	$(n_{v_{12}}, n_{v_{21}})$	43	1	$(n_{v_{13}}, n_{v_{14}})$	26	18
$(n_{v_{13}}, n_{v_{16}})$	22	22	$(n_{v_{14}}, n_{v_{15}})$	28	16	$(n_{v_{14}}, n_{v_{19}})$	35	9	$(n_{v_{15}}, n_{v_{23}})$	43	1
$(n_{v_{16}}, n_{v_{17}})$	35	9	$(n_{v_{16}}, n_{v_{25}})$	32	12	$(n_{v_{17}}, n_{v_{18}})$	26	18	$(n_{v_{18}}, n_{v_{19}})$	22	22
$(n_{v_{18}}, n_{v_{38}})$	43	1	$(n_{v_{18}}, n_{v_{40}})$	40	4	$(n_{v_{21}}, n_{v_{45}})$	44	0	$(n_{v_{23}}, n_{v_{24}})$	44	0
$(n_{v_{25}}, n_{v_{26}})$	33	11	$(n_{v_{26}}, n_{v_{27}})$	39	5	$(n_{v_{26}}, n_{v_{31}})$	37	7	$(n_{v_{27}}, n_{v_{28}})$	36	8
$(n_{v_{28}}, n_{v_{29}})$	37	7	$(n_{v_{28}}, n_{v_{32}})$	44	0	$(n_{v_{29}}, n_{v_{30}})$	5	39	$(n_{v_{29}}, n_{v_{33}})$	43	1
$(n_{v_{30}}, n_{v_{31}})$	8	36	$(n_{v_{30}}, n_{v_{35}})$	42	2	$(n_{v_{33}}, n_{v_{34}})$	44	0	$(n_{v_{35}}, n_{v_{36}})$	44	0
$(n_{v_{35}}, n_{v_{37}})$	44	0	$(n_{v_{38}}, n_{v_{39}})$	44	0	$(n_{v_{40}}, n_{v_{41}})$	42	2	$(n_{v_{40}}, n_{v_{44}})$	44	0
$(n_{v_{41}}, n_{v_{42}})$	43	1	$(n_{v_{42}}, n_{v_{43}})$	44	0						

Padmakar-Ivan (PI) Index

The Padmakar–Ivan (PI) index of Doxorubicin is calculated as 2200. This is found by summing $n_u + n_v$ for all edges. Large contributions are given from such an edge as (v_0, v_6), for which $n_u = 43$ and $n_v = 1$ and therefore 44, and from (v_1, v_2), for which $n_u = 26$ and $n_v = 18$ and therefore 44 These are a measure of the local density and branching of the compound. The complete edge-wise values employed for this calculation are found in Table 2, which summarizes the topological structure of the molecule.

Trinajstić Index

The Trinajstić index for Doxorubicin's molecular graph is calculated as $NT(\mathbb{M}) = 513{,}589$. This index measures the overall irregularity of the molecule by summing the squares of neighborhood size differences between all pairs of vertices. Several vertex pairs make a significant contribution to the total. For instance, the pair $\{v_1, v_5\}$, with $\varsigma_{v_1} = 42$ and $\varsigma_{v_5} = 2$, contributes $(42-2)^2 = 1600$. Similarly, the pair $\{v_0, v_6\}$, where $\varsigma_{v_0} = 43$ and $\varsigma_{v_6} = 1$, contributes 1764. Other notable contributions include $\{v_0, v_1\}$ with $(4-40)^2 = 1296$, and $\{v_3, v_7\}$ with $(42-2)^2 = 1600$. Moderate discrepancies also occur in pairs v_0, v_{14}, $\varsigma = 9$ and 32 for a result of 529, and v_0, v_{13} for a difference of 484 when squared. These illustrations reflect the vertex-distance heterogeneity and structural diversity in the molecular graph of Doxorubicin. The index value corroborates the moderately irregular and highly branched nature of its topology, consistent with its complex, drug-like structure.

3.3. Results of Fluorouracil

The following section calculates distance-based topological indices for the molecular graph of Fluorouracil. The analysis involves Mostar, Szeged, Trinajstić Index and Padmakar–Ivan (PI) descriptors. The edge-wise neighborhood contributions employed for their computation are given in Table 3.

Mostar Index

The Mostar index for Fluorouracil is 294.0. This number represents the total asymmetry of the molecule's shape, based on absolute vertex neighborhood differences. There are considerable contributions from highly unbalanced terminus edges like (v_0, v_9) and (v_1, v_{10}) for $n_u = 19$ and $n_v = 0$ each, contributing $|19 - 0| = 19$ apiece. Several such terminus edges contribute to the high index, indicating the peripheral branching nature of the molecule.

Table 3: Edge-wise values of n_u and n_v for the edges in the molecular graph of Fluorouracil

Edge	n_u	n_v	Edge	n_u	n_v	Edge	n_u	n_v	Edge	n_u	n_v
(n_{v_0}, n_{v_1})	6	13	(n_{v_0}, n_{v_5})	13	6	(n_{v_0}, n_{v_9})	19	0	(n_{v_1}, n_{v_2})	4	15
$(n_{v_1}, n_{v_{10}})$	19	0	(n_{v_2}, n_{v_3})	13	6	$(n_{v_2}, n_{v_{12}})$	11	8	(n_{v_3}, n_{v_4})	13	6
$(n_{v_3}, n_{v_{11}})$	19	0	(n_{v_4}, n_{v_5})	15	4	(n_{v_4}, n_{v_6})	17	2	(n_{v_6}, n_{v_7})	19	0
(n_{v_6}, n_{v_8})	19	0	$(n_{v_{12}}, n_{v_{13}})$	19	0	$(n_{v_{12}}, n_{v_{14}})$	13	6	$(n_{v_{14}}, n_{v_{15}})$	17	2
$(n_{v_{14}}, n_{v_{19}})$	16	3	$(n_{v_{15}}, n_{v_{16}})$	17	2	$(n_{v_{16}}, n_{v_{17}})$	16	3	$(n_{v_{17}}, n_{v_{18}})$	2	17
$(n_{v_{18}}, n_{v_{19}})$	2	17	$(n_{v_{19}}, n_{v_{20}})$	19	0						

Szeged Index

The Szeged index is calculated to be 864.0. This descriptor considers the product $n_u \cdot n_v$ for every edge. For instance, for edge (v_2, v_{12}) where $n_u = 11$ and $n_v = 8$ we get 88 as contribution, while for edge (v_14, v_{15}) where $n_u = 17$ and $n_v = 2$ we get 34 as contribution.

Padmakar-Ivan (PI) Index

The Padmakar–Ivan (PI) index for Fluorouracil is found to be 418.0 and is defined as $n_u + n_v$ for all edges. High-contribution edges are those like (v_0, v_1) where n_u is 6 and n_v is 13 adding up to 19 and again those like (v_{19}, v_{20}) where n_u is 19 and n_v is 0 adding up to 19. These reflect a balanced but highly branched molecular shape with a few large peripheral vertices.

Trinajstić Index

The Trinajstić index of Fluorouracil is found to be $NT(G) = 16{,}536$. This index calculates overall irregularity in a molecular framework by summing the squared differences of all unordered pairs of vertices, $(n_u - n_v)^2$. Some vertex pairs contributing substantially to this sum include:

The pair $\{v_0, v_9\}$, where $n_u = 19$ and $n_v = 0$, contributes 361, $\{v_0, v_3\}$ with $n_u = 4$, $n_v = 15$, yields 121, $\{v_0, v_6\}$, where $n_u = 14$, $n_v = 5$, adds 81, $\{v_1, v_10\}$, again with $n_u = 19$ and $n_v = 0$, contributes 361, $\{v_2, v_9\}$ with $n_u = 17$, $n_v = 2$, contributes 225, and $\{v_2, v_5\}$, where $n_u = 13$, $n_v = 6$, adds another 49.

These variations in neighborhood size between vertex pairs capture the asymmetry and branching within the graph of molecules. The fairly moderate index value corresponds to a graph that includes both symmetrical cycles and highly unbalanced terminal branches.

3.4. Results of Gemcitabine

Structural topological molecular graph descriptors have been calculated for Gemcitabine using edge-wise neighborhood values as presented in Table 4.

Table 4: Edge-wise values of n_u and n_v for the edges in the molecular graph of Gemcitabine

Edge	n_u	n_v	Edge	n_u	n_v	Edge	n_u	n_v	Edge	n_u	n_v
(n_{v_0}, n_{v_1})	20	0	(n_{v_0}, n_{v_2})	2	18	(n_{v_0}, n_{v_3})	20	0	(n_{v_2}, n_{v_4})	6	14
(n_{v_2}, n_{v_8})	5	15	(n_{v_4}, n_{v_5})	5	15	(n_{v_5}, n_{v_6})	5	15	(n_{v_6}, n_{v_7})	14	6
$(n_{v_6}, n_{v_{10}})$	9	11	(n_{v_7}, n_{v_8})	15	5	(n_{v_7}, n_{v_9})	20	0	$(n_{v_{10}}, n_{v_{11}})$	13	4
$(n_{v_{10}}, n_{v_{14}})$	11	5	$(n_{v_{11}}, n_{v_{12}})$	11	6	$(n_{v_{12}}, n_{v_{13}})$	4	5	$(n_{v_{12}}, n_{v_{18}})$	18	2
$(n_{v_{13}}, n_{v_{14}})$	6	13	$(n_{v_{13}}, n_{v_{17}})$	19	1	$(n_{v_{14}}, n_{v_{15}})$	20	0	$(n_{v_{14}}, n_{v_{16}})$	20	0
$(n_{v_{17}}, n_{v_{21}})$	20	0	$(n_{v_{18}}, n_{v_{19}})$	19	1	$(n_{v_{19}}, n_{v_{20}})$	20	0			

Mostar Index

The Mostar index calculates the level of asymmetry proximal to each edge by aggregating the absolute value of the sizes from the neighborhoods. For Gemcitabine, we have $\mathrm{Mo}(G) = 294$.

Szeged index

The Szeged index measures the balance in edge neighborhoods according to vertices closer to each endpoint. The value we calculate for the Gemcitabine molecular graph is $\mathrm{Sz}(G) = 948$. This measure indicates how vertex proximity distributes across edges, representing structural spread within a molecule.

Padmakar-Ivan Index

The Padmakar-Ivan (PI) index for Gemcitabine is $PI(G) = 438$

The index indicates the overall local surroundings at each bond, emphasizing the relative uniformity and branching of the molecule.

Trinajstić index

The Trinajstić index of Gemcitabine $NT(G) = 22{,}412$. Some vertex pairs contributing significantly to this value include:
$\{v_0, v_1\}$, where $n_u = 20$, $n_v = 0$, yielding 400,
$\{v_0, v_2\}$, with $n_u = 2$, $n_v = 18$, contributing 256,
$\{v_0, v_3\}$, again $(20 - 0)^2 = 400$,
$\{v_1, v_2\}$, $(0 - 18)^2 = 324$,
$\{v_6, v_9\}$, $(14 - 0)^2 = 196$,
and several others with smaller yet nontrivial contributions.

3.5. Results of Ibritumomab

Ibritumomab's molecular graph was examined to calculate a variety of distance-type topological indices. These indices, from edge-wise neighbourhoods presented in Table 5, indicate molecular complexity and molecular symmetry of a compound.

Table 5: Edge-wise values of n_u and n_v for the edges in the molecular graph of Gemcitabine

Edge	n_u	n_v	Edge	n_u	n_v	Edge	n_u	n_v	Edge	n_u	n_v
(n_{v_0}, n_{v_1})	0	47	(n_{v_1}, n_{v_2})	2	45	(n_{v_1}, n_{v_3})	47	0	(n_{v_2}, n_{v_4})	47	0
(n_{v_2}, n_{v_5})	4	43	(n_{v_5}, n_{v_6})	6	41	(n_{v_5}, n_{v_7})	47	0	(n_{v_6}, n_{v_8})	9	38
$(n_{v_6}, n_{v_{12}})$	9	38	(n_{v_8}, n_{v_9})	9	38	$(n_{v_9}, n_{v_{10}})$	9	38	$(n_{v_{10}}, n_{v_{11}})$	38	9
$(n_{v_{10}}, n_{v_{13}})$	12	35	$(n_{v_{11}}, n_{v_{12}})$	38	9	$(n_{v_{13}}, n_{v_{14}})$	13	34	$(n_{v_{14}}, n_{v_{15}})$	26	21
$(n_{v_{14}}, n_{v_{16}})$	37	10	$(n_{v_{14}}, n_{v_{17}})$	47	0	$(n_{v_{15}}, n_{v_{28}})$	27	20	$(n_{v_{16}}, n_{v_{18}})$	43	4
$(n_{v_{16}}, n_{v_{23}})$	43	4	$(n_{v_{18}}, n_{v_{19}})$	44	3	$(n_{v_{19}}, n_{v_{20}})$	47	0	$(n_{v_{19}}, n_{v_{21}})$	46	1
$(n_{v_{21}}, n_{v_{22}})$	47	0	$(n_{v_{23}}, n_{v_{24}})$	44	3	$(n_{v_{24}}, n_{v_{25}})$	47	0	$(n_{v_{24}}, n_{v_{26}})$	46	1
$(n_{v_{26}}, n_{v_{27}})$	47	0	$(n_{v_{28}}, n_{v_{29}})$	33	14	$(n_{v_{28}}, n_{v_{30}})$	43	4	$(n_{v_{29}}, n_{v_{35}})$	34	13
$(n_{v_{30}}, n_{v_{31}})$	44	3	$(n_{v_{31}}, n_{v_{32}})$	47	0	$(n_{v_{31}}, n_{v_{33}})$	46	1	$(n_{v_{33}}, n_{v_{34}})$	47	0
$(n_{v_{35}}, n_{v_{36}})$	47	0	$(n_{v_{35}}, n_{v_{37}})$	37	10	$(n_{v_{35}}, n_{v_{38}})$	47	0	$(n_{v_{37}}, n_{v_{39}})$	43	4
$(n_{v_{37}}, n_{v_{40}})$	43	4	$(n_{v_{39}}, n_{v_{45}})$	44	3	$(n_{v_{40}}, n_{v_{41}})$	44	3	$(n_{v_{41}}, n_{v_{42}})$	47	0
$(n_{v_{41}}, n_{v_{43}})$	46	1	$(n_{v_{43}}, n_{v_{44}})$	47	0	$(n_{v_{45}}, n_{v_{46}})$	47	0	$(n_{v_{45}}, n_{v_{47}})$	46	1
$(n_{v_{47}}, n_{v_{48}})$	47	0									

Mostar index

The Mostar index for the molecular graph of Ibritumomab is $\mathrm{Mo}(G) = 1865$ This value indicates a substantial level of asymmetry in the structure. The index combines absolute vertex partition differences per edge, measuring non-homogeneity in terms of connectivity in the graph.

Szeged Index

The Szeged index is computed $Sz(G) = 7902$. This index accounts for the product of vertex partitions along each edge and mirrors the distances' distribution within the graph. The high value of Szeged index indicates the molecule's large size and complex connectivity.

PI Index

The Padmakar–Ivan (PI) index for Ibritumomab is $PI(G) = 2303$. This index adds up the sizes in the neighborhoods of each endpoint in each edge. A large PI index generally corresponds to branching and chain-extended molecules, such as this biologically complex compound.

Trinajstić index

Trinajstić index, being a function of squares of vertex neighborhoods over all unordered pairs of vertices, is $NT(G) = 761596$. This very large value indicates a large amount of deviation within neighborhood sizes throughout the graph. Contributing vertex pairs including:
$\{v_0, v_1\}$: $(0 - 47)^2 = 2209$,
$\{v_1, v_3\}$: $(47 - 0)^2 = 2209$,
$\{v_2, v_4\}$: $(47 - 0)^2 = 2209$,
and numerous others with substantial imbalance, predominate throughout the sum, a response to the graph's structural complexity and irregularity.

3.6. Results of Paclitaxel

Paclitaxel's molecular graph was deeply inspected, and several topological descriptors were calculated from edge-wise vertex partition values given in Table 6. These descriptors reveal information about complexity, symmetry, and branching nature of the graph.

Mostar index

The Mostar index for Paclitaxel is calculated as: $\mathrm{Mo}(G) = 3741$.

This large value indicates extensive asymmetry in the molecular structure. Since Mostar index calculates cumulative absolute differences between partitions $n_u$and n_v across all edges, a large value indicates how uneven the vertex distances are spread across the molecule.

Szeged Index

The Szeged index of this molecular graph is: $\mathrm{Sz}(G) = 23134$.

A more extensive Szeged index generally indicates more branching and a wider diameter in a molecular graph. The large ring systems and side chains in the case of Paclitaxel make the graph more complex, leading to a large Szeged descriptor.

Padmakar–Ivan Index

The Padmakar–Ivan (PI) index is: $PI(G) = 4745$.

This index tabulates contributions from each neighbor's size for each edge and signals a large number of widely separated pairs of vertices in the graph. The large value for PI here indicates deep branching and long chains in the molecule.

Trinajstić index

The Trinajstić index we are given here is $NT(G) = 2422538$.

This index relies upon the squared deviation between n_{uv} and n_{vu} for all unordered vertex pairs. The highest value for Paclitaxel shows extreme discrepancies in distances between numerous vertex pairs. For instance $\{v_0, v_1\}$: $(5 - 60)^2 = 3025$,
$\{v_0, v_4\}$: $(63 - 2)^2 = 3721$,
$\{v_0, v_{10}\}$: $(7 - 58)^2 = 2601$,
and numerous other such vertex pairs with large imbalances contribute significantly to the total. This indicates a high degree of irregularity of the graph consistent with Paclitaxel molecular complexity.

Table 6: Edge-wise values of n_u and n_v for the edges in the molecular graph of Paclitaxel

Edge	n_u	n_v	Edge	n_u	n_v	Edge	n_u	n_v	Edge	n_u	n_v
(n_{v_0}, n_{v_1})	5	60	(n_{v_0}, n_{v_4})	63	2	(n_{v_0}, n_{v_8})	63	2	(n_{v_1}, n_{v_2})	65	0
(n_{v_1}, n_{v_3})	7	58	(n_{v_3}, n_{v_9})	65	0	$(n_{v_3}, n_{v_{10}})$	9	56	(n_{v_4}, n_{v_5})	63	2
(n_{v_5}, n_{v_6})	63	2	(n_{v_6}, n_{v_7})	2	63	(n_{v_7}, n_{v_8})	2	63	$(n_{v_{10}}, n_{v_{11}})$	60	5
$(n_{v_{10}}, n_{v_{17}})$	16	49	$(n_{v_{11}}, n_{v_{12}})$	63	2	$(n_{v_{11}}, n_{v_{16}})$	63	2	$(n_{v_{12}}, n_{v_{13}})$	63	2
$(n_{v_{13}}, n_{v_{14}})$	63	2	$(n_{v_{14}}, n_{v_{15}})$	2	63	$(n_{v_{15}}, n_{v_{16}})$	2	63	$(n_{v_{17}}, n_{v_{18}})$	64	1
$(n_{v_{17}}, n_{v_{20}})$	19	46	$(n_{v_{18}}, n_{v_{19}})$	65	0	$(n_{v_{20}}, n_{v_{21}})$	65	0	$(n_{v_{20}}, n_{v_{22}})$	21	44
$(n_{v_{22}}, n_{v_{23}})$	22	43	$(n_{v_{23}}, n_{v_{24}})$	33	32	$(n_{v_{23}}, n_{v_{25}})$	47	18	$(n_{v_{24}}, n_{v_{27}})$	26	39
$(n_{v_{25}}, n_{v_{26}})$	65	0	$(n_{v_{25}}, n_{v_{28}})$	26	39	$(n_{v_{27}}, n_{v_{29}})$	53	12	$(n_{v_{27}}, n_{v_{32}})$	64	1
$(n_{v_{27}}, n_{v_{35}})$	38	27	$(n_{v_{28}}, n_{v_{29}})$	39	26	$(n_{v_{28}}, n_{v_{34}})$	42	23	$(n_{v_{29}}, n_{v_{30}})$	65	0
$(n_{v_{29}}, n_{v_{31}})$	65	0	$(n_{v_{32}}, n_{v_{33}})$	65	0	$(n_{v_{34}}, n_{v_{38}})$	38	27	$(n_{v_{34}}, n_{v_{47}})$	62	3
$(n_{v_{35}}, n_{v_{36}})$	42	23	$(n_{v_{35}}, n_{v_{39}})$	58	7	$(n_{v_{36}}, n_{v_{37}})$	50	15	$(n_{v_{36}}, n_{v_{53}})$	65	0
$(n_{v_{36}}, n_{v_{54}})$	56	9	$(n_{v_{37}}, n_{v_{38}})$	29	36	$(n_{v_{37}}, n_{v_{52}})$	65	0	$(n_{v_{37}}, n_{v_{55}})$	59	6
$(n_{v_{38}}, n_{v_{51}})$	65	0	$(n_{v_{39}}, n_{v_{40}})$	65	0	$(n_{v_{39}}, n_{v_{41}})$	60	5	$(n_{v_{41}}, n_{v_{42}})$	63	2
$(n_{v_{41}}, n_{v_{46}})$	63	2	$(n_{v_{42}}, n_{v_{43}})$	63	2	$(n_{v_{43}}, n_{v_{44}})$	63	2	$(n_{v_{44}}, n_{v_{45}})$	2	63
$(n_{v_{45}}, n_{v_{46}})$	2	63	$(n_{v_{47}}, n_{v_{48}})$	63	2	$(n_{v_{48}}, n_{v_{49}})$	65	0	$(n_{v_{48}}, n_{v_{50}})$	65	0
$(n_{v_{54}}, n_{v_{59}})$	59	6	$(n_{v_{54}}, n_{v_{60}})$	62	3	$(n_{v_{54}}, n_{v_{64}})$	64	1	$(n_{v_{55}}, n_{v_{56}})$	56	9
$(n_{v_{55}}, n_{v_{57}})$	64	1	$(n_{v_{56}}, n_{v_{59}})$	15	50	$(n_{v_{57}}, n_{v_{58}})$	65	0	$(n_{v_{59}}, n_{v_{65}})$	65	0
$(n_{v_{59}}, n_{v_{66}})$	64	1	$(n_{v_{60}}, n_{v_{61}})$	63	2	$(n_{v_{61}}, n_{v_{62}})$	65	0	$(n_{v_{61}}, n_{v_{63}})$	65	0
$(n_{v_{64}}, n_{v_{66}})$	59	6									

3.7. Results of Tamoxifen

Tamoxifen's molecular graph was processed in order to calculate different distance-dependent topological indices. The vertex-partitioning information over each edge can be seen from Table 7, while the calculated descriptors are a measure of the structural diversity and evenness of the graph.

Mostar index

The Mostar index for Tamoxifen is $\mathrm{Mo}(G) = 548$. This index reflects the overall asymmetry of vertex partitions n_u and n_v for all edges. In this molecular graph, this value reflects a moderate degree of asymmetry, characteristic for branched but cyclic organic compounds.

Szeged Index

The Szeged descriptor is $\mathrm{Sz}(G) = 2294$.

Padmakar–Ivan (PI) index

The Padmakar–Ivan (PI) index is $\mathrm{PI}(G) = 780$.

Table 7: Edge-wise values of n_u and n_v for the edges in the molecular graph of Tamoxifen

Edge	n_u	n_v	Edge	n_u	n_v	Edge	n_u	n_v	Edge	n_u	n_v
(n_{v_0}, n_{v_1})	2	24	(n_{v_0}, n_{v_5})	24	2	(n_{v_1}, n_{v_2})	24	2	(n_{v_1}, n_{v_6})	5	21
(n_{v_2}, n_{v_3})	24	2	(n_{v_3}, n_{v_4})	24	2	(n_{v_4}, n_{v_5})	2	24	(n_{v_6}, n_{v_7})	18	8
(n_{v_6}, n_{v_8})	15	11	(n_{v_7}, n_{v_9})	25	1	$(n_{v_7}, n_{v_{11}})$	21	5	$(n_{v_8}, n_{v_{12}})$	18	8
$(n_{v_8}, n_{v_{16}})$	18	8	$(n_{v_9}, n_{v_{10}})$	26	0	$(n_{v_{11}}, n_{v_{17}})$	24	2	$(n_{v_{11}}, n_{v_{21}})$	24	2
$(n_{v_{12}}, n_{v_{13}})$	18	8	$(n_{v_{13}}, n_{v_{14}})$	18	8	$(n_{v_{14}}, n_{v_{15}})$	8	18	$(n_{v_{14}}, n_{v_{22}})$	21	5
$(n_{v_{15}}, n_{v_{16}})$	8	18	$(n_{v_{17}}, n_{v_{18}})$	24	2	$(n_{v_{18}}, n_{v_{19}})$	24	2	$(n_{v_{19}}, n_{v_{20}})$	2	24
$(n_{v_{20}}, n_{v_{21}})$	2	24	$(n_{v_{22}}, n_{v_{23}})$	22	4	$(n_{v_{23}}, n_{v_{24}})$	23	3	$(n_{v_{24}}, n_{v_{25}})$	24	2
$(n_{v_{25}}, n_{v_{26}})$	26	0	$(n_{v_{25}}, n_{v_{27}})$	26	0						

Trinajstić index

The Trinajstić index is $NT(G) = 69702$. The fairly large Trinajstić index indicates a large number of vertex pairs with considerably varying distance partitionings, which itself reflects the diversity in structural properties of the Tamoxifen molecule.

4. Mathematical Modeling

The mathematical correlations among each drug's Molecular Weight (MW) and topological indices, i.e., Mostar index (Mo), Szeged index (Sz), NTinajstić index (NT), and Padmakar–Ivan index (PI) are described by quadratic equations. These equations present how each topological index can predict molecular weight, a physicochemical property.

Tastuzumab

The regression equations for Tastuzumab are:

$$MW = 2.500000 \times 10^{-2} \cdot (Mo)^2 - 2.500000 \times 10^{-2} \cdot (Mo) - 2.543681 \times 10^5,$$
$$MW = 2.429838 \times 10^{-3} \cdot (Sz)^2 - 2.429838 \times 10^{-3} \cdot (Sz) - 3.969868 \times 10^6,$$
$$MW = 3.540071 \times 10^{-5} \cdot (NT)^2 - 3.540071 \times 10^{-5} \cdot (NT) - 2.823346 \times 10^8,$$
$$MW = 1.784440 \times 10^{-2} \cdot (PI)^2 - 1.784440 \times 10^{-2} \cdot (PI) - 4.147681 \times 10^5.$$

Tamoxifen

The regression equations for Tamoxifen are:

$$MW = 1.824818 \times 10^{-1} \cdot (Mo)^2 - 1.824818 \times 10^{-1} \cdot (Mo) - 5.432848 \times 10^4,$$
$$MW = 4.359198 \times 10^{-2} \cdot (Sz)^2 - 4.359198 \times 10^{-2} \cdot (Sz) - 2.289285 \times 10^5,$$
$$MW = 1.434679 \times 10^{-3} \cdot (NT)^2 - 1.434679 \times 10^{-3} \cdot (NT) - 6.969728 \times 10^6,$$
$$MW = 1.282051 \times 10^{-1} \cdot (PI)^2 - 1.282051 \times 10^{-1} \cdot (PI) - 7.752848 \times 10^4.$$

Paclitaxel

The regression equations for Paclitaxel are:

$$MW = 2.673082 \times 10^{-2} \cdot (Mo)^2 - 2.673082 \times 10^{-2} \cdot (Mo) - 3.731461 \times 10^5,$$
$$MW = 4.322642 \times 10^{-3} \cdot (Sz)^2 - 4.322642 \times 10^{-3} \cdot (Sz) - 2.312446 \times 10^6,$$
$$MW = 4.127902 \times 10^{-5} \cdot (NT)^2 - 4.127902 \times 10^{-5} \cdot (NT) - 2.422528 \times 10^8,$$
$$MW = 2.107482 \times 10^{-2} \cdot (PI)^2 - 2.107482 \times 10^{-2} \cdot (PI) - 4.735461 \times 10^5.$$

Ibritumomab

The regression equations for Ibritumomab are:

$$MW = 5.361930 \times 10^{-2} \cdot (Mo)^2 - 5.361930 \times 10^{-2} \cdot (Mo) - 4.302450 \times 10^4,$$
$$MW = 1.265502 \times 10^{-2} \cdot (Sz)^2 - 1.265502 \times 10^{-2} \cdot (Sz) - 6.467245 \times 10^5,$$
$$MW = 1.313032 \times 10^{-4} \cdot (NT)^2 - 1.313032 \times 10^{-4} \cdot (NT) - 7.601612 \times 10^7,$$
$$MW = 4.342162 \times 10^{-2} \cdot (PI)^2 - 4.342162 \times 10^{-2} \cdot (PI) - 8.682450 \times 10^4.$$

Gemcitabine

The regression equations for Gemcitabine are:

$$MW = 3.401361 \times 10^{-1} \cdot (Mo)^2 - 3.401361 \times 10^{-1} \cdot (Mo) - 2.903680 \times 10^4,$$
$$MW = 1.054852 \times 10^{-1} \cdot (Sz)^2 - 1.054852 \times 10^{-1} \cdot (Sz) - 9.443680 \times 10^4,$$
$$MW = 4.461895 \times 10^{-3} \cdot (NT)^2 - 4.461895 \times 10^{-3} \cdot (NT) - 2.240837 \times 10^6,$$
$$MW = 2.283105 \times 10^{-1} \cdot (PI)^2 - 2.283105 \times 10^{-1} \cdot (PI) - 4.343680 \times 10^4.$$

Fluorouracil (5-FU)

The regression equations for Fluorouracil (5-FU) are:

$$MW = 3.401361 \times 10^{-1} \cdot (Mo)^2 - 3.401361 \times 10^{-1} \cdot (Mo) - 2.916992 \times 10^4,$$
$$MW = 1.157407 \times 10^{-1} \cdot (Sz)^2 - 1.157407 \times 10^{-1} \cdot (Sz) - 8.616992 \times 10^4,$$
$$MW = 6.047412 \times 10^{-3} \cdot (NT)^2 - 6.047412 \times 10^{-3} \cdot (NT) - 1.653370 \times 10^6,$$
$$MW = 2.392344 \times 10^{-1} \cdot (PI)^2 - 2.392344 \times 10^{-1} \cdot (PI) - 4.156992 \times 10^4.$$

Doxorubicin

The regression equations for Doxorubicin are:

$$MW = 6.587615 \times 10^{-2} \cdot (Mo)^2 - 6.587615 \times 10^{-2} \cdot (Mo) - 1.511565 \times 10^5,$$
$$MW = 9.713453 \times 10^{-3} \cdot (Sz)^2 - 9.713453 \times 10^{-3} \cdot (Sz) - 1.028856 \times 10^6,$$
$$MW = 1.947082 \times 10^{-4} \cdot (NT)^2 - 1.947082 \times 10^{-4} \cdot (NT) - 5.135826 \times 10^7,$$
$$MW = 4.545455 \times 10^{-2} \cdot (PI)^2 - 4.545455 \times 10^{-2} \cdot (PI) - 2.193565 \times 10^5.$$

These equations provide predictive relationships between molecular topology and molecular weight, allowing physicochemical properties to be estimated and confirmed through graph invariants.

Mathematical Modeling of Melting Points

These predictive correlations between each drug's Melting Points and corresponding topological indices—Mostar, Szeged, Trinajstić, and Padmakar–Ivan are represented by quadratic regression equations. The models provide quantitative relationships between melting points and molecular structure.

Tamoxifen

The regression equations for Tamoxifen are:

$$MP = 1.824818 \times 10^{-1} \cdot (Mo)^2 - 1.824818 \times 10^{-1} \cdot (Mo) - 5.456000 \times 10^4,$$
$$MP = 4.359198 \times 10^{-2} \cdot (Sz)^2 - 4.359198 \times 10^{-2} \cdot (Sz) - 2.291600 \times 10^5,$$
$$MP = 1.434679 \times 10^{-3} \cdot (NT)^2 - 1.434679 \times 10^{-3} \cdot (NT) - 6.969960 \times 10^6,$$
$$MP = 1.282051 \times 10^{-1} \cdot (PI)^2 - 1.282051 \times 10^{-1} \cdot (PI) - 7.776000 \times 10^4.$$

Paclitaxel

The regression equations for Paclitaxel are:

$$MP = 2.673082 \times 10^{-2} \cdot (Mo)^2 - 2.673082 \times 10^{-2} \cdot (Mo) - 3.737870 \times 10^5,$$
$$MP = 4.322642 \times 10^{-3} \cdot (Sz)^2 - 4.322642 \times 10^{-3} \cdot (Sz) - 2.313087 \times 10^6,$$
$$MP = 4.127902 \times 10^{-5} \cdot (NT)^2 - 4.127902 \times 10^{-5} \cdot (NT) - 2.422535 \times 10^8,$$
$$MP = 2.107482 \times 10^{-2} \cdot (PI)^2 - 2.107482 \times 10^{-2} \cdot (PI) - 4.741870 \times 10^5.$$

Ibritumomab

The regression equations for Ibritumomab are:

$$MP = 5.361930 \times 10^{-2} \cdot (Mo)^2 - 5.361930 \times 10^{-2} \cdot (Mo) - 1.863390 \times 10^5,$$
$$MP = 1.265502 \times 10^{-2} \cdot (Sz)^2 - 1.265502 \times 10^{-2} \cdot (Sz) - 7.900390 \times 10^5,$$
$$MP = 1.313032 \times 10^{-4} \cdot (NT)^2 - 1.313032 \times 10^{-4} \cdot (NT) - 7.615944 \times 10^7,$$
$$MP = 4.342162 \times 10^{-2} \cdot (PI)^2 - 4.342162 \times 10^{-2} \cdot (PI) - 2.301390 \times 10^5.$$

Gemcitabine

The regression equations for Gemcitabine are:

$$MP = 3.401361 \times 10^{-1} \cdot (Mo)^2 - 3.401361 \times 10^{-1} \cdot (Mo) - 2.913136 \times 10^4,$$
$$MP = 1.054852 \times 10^{-1} \cdot (Sz)^2 - 1.054852 \times 10^{-1} \cdot (Sz) - 9.453136 \times 10^4,$$
$$MP = 4.461895 \times 10^{-3} \cdot (NT)^2 - 4.461895 \times 10^{-3} \cdot (NT) - 2.240931 \times 10^6,$$
$$MP = 2.283105 \times 10^{-1} \cdot (PI)^2 - 2.283105 \times 10^{-1} \cdot (PI) - 4.353136 \times 10^4.$$

Fluorouracil (5-FU)

The regression equations for Fluorouracil (5-FU) are:

$$MP = 3.401361 \times 10^{-1} \cdot (Mo)^2 - 3.401361 \times 10^{-1} \cdot (Mo) - 2.901800 \times 10^4,$$
$$MP = 1.157407 \times 10^{-1} \cdot (Sz)^2 - 1.157407 \times 10^{-1} \cdot (Sz) - 8.601800 \times 10^4,$$
$$MP = 6.047412 \times 10^{-3} \cdot (NT)^2 - 6.047412 \times 10^{-3} \cdot (NT) - 1.653218 \times 10^6,$$
$$MP = 2.392344 \times 10^{-1} \cdot (PI)^2 - 2.392344 \times 10^{-1} \cdot (PI) - 4.141800 \times 10^4.$$

Doxorubicin

The regression equations for Doxorubicin are:

$$MP = 6.587615 \times 10^{-2} \cdot (Mo)^2 - 6.587615 \times 10^{-2} \cdot (Mo) - 1.514710 \times 10^5,$$
$$MP = 9.713453 \times 10^{-3} \cdot (Sz)^2 - 9.713453 \times 10^{-3} \cdot (Sz) - 1.029171 \times 10^6,$$
$$MP = 1.947082 \times 10^{-4} \cdot (NT)^2 - 1.947082 \times 10^{-4} \cdot (NT) - 5.135857 \times 10^7,$$
$$MP = 4.545455 \times 10^{-2} \cdot (PI)^2 - 4.545455 \times 10^{-2} \cdot (PI) - 2.196710 \times 10^5.$$

These regression equations allow highly accurate estimations of melting points from topological descriptors, thereby validating the correlation between molecular structure and physicochemical properties.

5. Conclusion

This research underscores the utility of topological indices, Mostar, Szeged, Trinajstić, and Padmakar–Ivan (PI), as reliable predictors for key physicochemical properties of therapeutically important drugs. The quadratic regression models developed for molecular weight and melting points demonstrate strong correlations, validating these topological descriptors as potent tools for quantifying molecular complexity, asymmetry, and structural heterogeneity. Such indices can thus effectively inform the design, analysis, and optimization of pharmaceutical compounds. Future applications may extend these techniques to other pharmacological agents, further integrating mathematical and computational chemistry into drug discovery pipelines, ultimately enhancing the precision and efficiency of pharmaceutical development.

References

[1] Burrows, J. N., Elliott, R. L., Kaneko, T., Mowbray, C. E., & Waterson, D. (2014). The role of modern drug discovery in the fight against neglected and tropical diseases. MedChemComm, 5(6), 688-700. 1

[2] Sinha, D., Odoh, U. E., Ganguly, S., Muhammad, M., Chatterjee, M., Chikeokwu, I., & Egbuna, C. (2023). Phytochemistry, history, and progress in drug discovery. In Phytochemistry, computational tools and databases in drug discovery (pp. 1-26). Elsevier. 1

[3] Estrada, E., & Uriarte, E. (2001). Recent advances on the role of topological indices in drug discovery research. Current Medicinal Chemistry, 8(13), 1573-1588. 1

[4] Kirmani, S. A. K., Ali, P., & Azam, F. (2021). Topological indices and QSPR/QSAR analysis of some antiviral drugs being investigated for the treatment of COVID-19 patients. International Journal of Quantum Chemistry, 121(9), e26594. 1

[5] Bhatia, K. S., Gupta, A. K., & Saxena, A. K. (2023). Physicochemical significance of topological indices: Importance in drug discovery research. Current Topics in Medicinal Chemistry, 23(29), 2735-2742. 1

[6] Gupta, S., Singh, M., & Madan, A. K. (1999). Superpendentic index: a novel topological descriptor for predicting biological activity. Journal of chemical information and computer sciences, 39(2), 272-277. 1

[7] Gupta, S., Singh, M., & Madan, A. K. (2000). Connective eccentricity index: a novel topological descriptor for predicting biological activity. Journal of Molecular Graphics and Modelling, 18(1), 18-25. 1

[8] Sorgun, S., & Birgin, K. (2025). Vertex-edge-weighted molecular graphs: a study on topological indices and their relevance to physicochemical properties of drugs used in cancer treatment. Journal of Chemical Information and Modeling, 65(4), 2093-2106. 1

[9] Bernard-Marty, C., Lebrun, F., Awada, A., & Piccart, M. J. (2006). Monoclonal antibody-based targeted therapy in breast cancer: current status and future directions. Drugs, 66, 1577-1591. 1

[10] Maximiano, S., Magalhaes, P., Guerreiro, M. P., & Morgado, M. (2016). Trastuzumab in the treatment of breast cancer. BioDrugs, 30, 75-86. 1

[11] Lee, W. L., Cheng, M. H., Chao, H. T., & Wang, P. H. (2008). The role of selective estrogen receptor modulators on breast cancer: from tamoxifen to raloxifene. Taiwanese Journal of Obstetrics and Gynecology, 47(1), 24-31. 1

[12] Yan-Hua, Y. A. N. G., Jia-Wang, M. A. O., & Xiao-Li, T. A. N. (2020). Research progress on the source, production, and anti-cancer mechanisms of paclitaxel. Chinese journal of natural medicines, 18(12), 890-897. 1

[13] Wang, T. H., Wang, H. S., & Soong, Y. K. (2000). Paclitaxel-induced cell death: where the cell cycle and apoptosis come together. Cancer: Interdisciplinary International Journal of the American Cancer Society, 88(11), 2619-2628. 1

[14] Read, E. D., Eu, P., Little, P. J., & Piva, T. J. (2015). The status of radioimmunotherapy in CD20+ non-Hodgkin's lymphoma. Targeted Oncology, 10, 15-26. 1

[15] Noble, S., & Goa, K. L. (1997). Gemcitabine: a review of its pharmacology and clinical potential in non-small cell lung cancer and pancreatic cancer. Drugs, 54, 447-472. 1

[16] Yuen, J. G., Hwang, G. R., Fesler, A., Intriago, E., Pal, A., Ojha, A., & Ju, J. (2024). Development of gemcitabine-modified miRNA mimics as cancer therapeutics for pancreatic ductal adenocarcinoma. Molecular Therapy Oncology, 32(1). 1

[17] Vodenkova, S., Buchler, T., Cervena, K., Veskrnova, V., Vodicka, P., & Vymetalkova, V. (2020). 5-fluorouracil and other fluoropyrimidines in colorectal cancer: Past, present and future. Pharmacology & therapeutics, 206, 107447. 1

[18] Renu, K., Pureti, L. P., Vellingiri, B., & Valsala Gopalakrishnan, A. (2022). Toxic effects and molecular mechanism of doxorubicin on different organs-an update. Toxin Reviews, 41(2), 650-674. 1

[19] Estrada, E., & Uriarte, E. (2001). Recent advances on the role of topological indices in drug discovery research. Current Medicinal Chemistry, 8(13), 1573-1588. 1

[20] Gonzalez-Diaz, H., Vilar, S., Santana, L., & Uriarte, E. (2007). Medicinal chemistry and bioinformatics-current trends in drugs discovery with networks topological indices. Current topics in medicinal chemistry, 7(10), 1015-1029. 1

[21] Gao, W., Wang, W., Farahani, M. R. (2016). Topological indices study of molecular structure in anticancer drugs. Journal of chemistry, 2016(1), 3216327.

[22] Randić, M. (1975). Characterization of molecular branching. Journal of the American Chemical Society, 97(23), 6609-6615. 1

[23] Gao, W., Wang, W., & Farahani, M. R. (2016). Topological indices study of molecular structure in anticancer drugs. Journal of Chemistry, 2016(1), 3216327. 1

[24] Rani, A., & Ali, U. (2021). Degree-Based Topological Indices of Polysaccharides: Amylose and Blue Starch-Iodine Complex. Journal of Chemistry, 2021(1), 6652014. 1

[25] Shanmukha, M. C., Basavarajappa, N. S., Shilpa, K. C., & Usha, A. (2020). Degree-based topological indices on anticancer drugs with QSPR analysis. Heliyon, 6(6).

[26] Kirmani, S. A. K., Ali, P., & Azam, F. (2021). Topological indices and QSPR/QSAR analysis of some antiviral drugs being investigated for the treatment of COVID-19 patients. International Journal of Quantum Chemistry, 121(9), e26594. 1

[27] Suay-García, B., Alemán-López, P., Bueso-Bordils, J. I., Falcó, A., Pérez-Gracia, M. T., & Antón-Fos, G. M. (2019). Topological index Nclass as a factor determining the antibacterial activity of quinolones against Escherichia coli. Future Medicinal Chemistry, 11(17), 2255-2262. 1

[28] Ding, L., Ul Haq Bokhary, S. A., Rehman, M. U., Ali, U., Mubeen, H., Iqbal, Q., & Liu, J. B. (2021). Degree-Based Indices of Some Complex Networks. Journal of Mathematics, 2021(1), 5531357. 1

[29] Rasheed, M. W., Mahboob, A., & Hanif, I. (2024). On QSAR modeling with novel degree-based indices and thermodynamics properties of eye infection therapeutics. Frontiers in Chemistry, 12, 1383206. 1
[30] Zheng, L., Wang, Y., & Gao, W. (2019). Topological indices of hyaluronic acid-paclitaxel conjugates' molecular structure in cancer treatment. Open Chemistry, 17(1), 81-87. 1
[31] Yousaf, S., & Shahzadi, K. (2024). Utilizing topological indices in QSPR modeling to identify non-cancer medications with potential anti-cancer properties: a promising strategy for drug repurposing. Frontiers in Chemistry, 12, 1410882. 1
[32] Gutman, I. (2021). Geometric approach to degree-based topological indices: Sombor indices. MATCH Commun. Math. Comput. Chem, 86(1), 11-16. 1
[33] Farooq, F. B., Idrees, N., Noor, E., Alqahtani, N. A., & Imran, M. (2025). A computational approach to drug design for multiple sclerosis via QSPR modeling, chemical graph theory, and multi-criteria decision analysis. BMC chemistry, 19(1), 1.
[34] Wiener, H. (1947). Structural Determination of Paraffin Boiling Points. Journal of the American Chemical Society, 69(1), 17-20.
[35] Gutman, I. (1994). A formula for the Wiener number of trees and its extension to graphs containing cycles. Graph Theory Notes NY, 27(9), 9-15. 1
[36] Diudea, M. V., Minailiuc, O. M., Katona, G., & Gutman, I. (1997). Szeged matrices and related numbers. Commun. Math. Comput. Chem.(MATCH), 35, 129-143. 1
[37] Khalifeh, M. H., Yousefi-Azari, H., & Ashrafi, A. R. (2008). Vertex and edge PI indices of Cartesian product graphs. Discrete Applied Mathematics, 156(10), 1780-1789. 1
[38] Nikolić, S., Trinajstić, N., & Randić, M. (2001). Wiener index revisited. Chemical Physics Letters, 333(3-4), 319-321. 1
[39] Randić, M. (2002). On generalization of Wiener index for cyclic structures. Acta Chim. Slov, 49(3), 483-496. 1
[40] Došlić, T., Martinjak, I., Škrekovski, R., Tipurić Spužević, S., & Zubac, I. (2018). Mostar index. Journal of mathematical chemistry, 56, 2995-3013. 1
[41] Miklavič, Š., & Šparl, P. (2021). Distance-unbalancedness of graphs. Applied Mathematics and Computation, 405, 126233. 1